Self-induced gap solitons in nonlinear magnetic metamaterials

Weina Cui,[1,2] Yongyuan Zhu,[1,*] Hongxia Li,[2] and Sumei Liu[2]
[1]*National Laboratory of Solid State Microstructures, Nanjing University, Nanjing 210093, People's Republic of China*
[2]*Department of Applied Physics, Nanjing University of Science and Technology, Nanjing 210094, People's Republic of China*
(Received 8 May 2009; published 30 September 2009)

The self-induced gap solitons in nonlinear magnetic metamaterials is investigated. It is shown that the self-induced gap solitons may exist due to the interaction of the discreteness and nonlinearity. The evolution of these localized structures is studied in the phase plane and analytical and numerical expressions are obtained.

DOI: 10.1103/PhysRevE.80.036608 PACS number(s): 41.20.Jb, 63.20.Pw, 75.30.Kz, 78.20.Ci

I. INTRODUCTION

The formation and dynamics of localized structures in nonlinear discrete systems have been the subject of intense investigation theoretically and experimentally [1]. The systems include anharmonic crystals, conducting polymer chains, Heisenberg ferromagnetic chains, Josephson-junction arrays, and photonic lattices, etc. [2–5]. The localized structures result from the interplay between nonlinearity and discreteness that have no counterpart whatsoever in continuous systems. Gap solitons as one type of localized modes attracts much attention since it was first introduced by Chen and Mills when they studied the nonlinear optical response of superlattices [6]. For one-dimensional system Kivshar proposed a self-induced lattice gap soliton theory which shows that localized structures may appear due to a nonlinearity-induced symmetry breaking between two equivalent eigenmodes [7].

Since split ring resonators (SRRs) were proposed and applied to design artificial media with negative permeability [8,9], many researchers became interested in the properties of these magnetic metamaterials (MMs) [10]. The MMs not only exhibit magnetic properties unavailable in naturally occurring materials but also support a type of guided waves, called magnetoinductive (MI) waves, which owe their existence to magnetic coupling between the elements [11,12]. The controllable parameters of each engineering elements provide great flexibility to design arrays with quite different intrinsic properties. Moreover, either by embedding the SRRs in a Kerr-type medium [13,14] or by inserting certain nonlinear elements (e.g., diodes) in each SRR [15–17], MMs may take on nonlinear properties. The combination of nonlinearity and discreteness allows one to expect the formation of nonlinear localized structure in MMs. Recent researches show one-dimensional (1D) or two-dimensional (2D) discrete array of nonlinear SRRs supports localized structures in the form of discrete breathers [18,19], magnetic domain walls [20], and magnetoinductive envelope solitons [21]. However, to the author's knowledge, gap solitons as one of localized structures are not reported up to now in nonlinear SRR arrays.

In this paper, we consider the propagation of a weakly nonlinear charge variation in 1D MMs formed by a discrete array of nonlinear SRRs where each element coupled magnetically to its nearest neighbors. The description for the charge stored in SRR involves a set of difference-differential equations and the discreteness makes the properties of the system periodic. Due to the interplay between discreteness and nonlinearity types of nonlinear excitations may be possible in 1D nonlinear SRR arrays. To obtain the nonlinear excitations, we use a systematic method called the quasidiscreteness approximation. It will be shown analytically and numerically that self-induced gap solitons may exist as a result of nonlinearity-induced gap in the continuum spectrum.

II. PHYSICAL MODEL

Here we consider 1D discrete, periodic arrays of N identical nonlinear SRRs with their centers separated by distance d_0. A 1D array can be constructed either in the planar configuration or in the axial configuration [12]. The nonlinearity arises from a Kerr-type dielectric which fills the SRR slits [13]. Equivalent permittivity is $\epsilon(|E|^2)=\epsilon_0(\epsilon_l+\alpha|E|^2/E_c^2)$ depending on the electric field E, where ϵ_0 and ϵ_l represent the vacuum permittivity and linear permittivity, respectively, E_c is a characteristic electric field, and $\alpha=+1(\alpha=-1)$ accounts for self-focusing (defocusing) nonlinearity. Each SRR can be modeled as a nonlinear resistor-inductor-capacitor (RLC) circuit driven by an alternating voltage source, with Ohmic resistance R, self-inductance L, and nonlinear capacitance C. SRRs are coupled weakly to its nearest neighbors due to magnetic interactions through their mutual inductance M. For planar configurations, the nearest-neighbor approximation is valid even if the SRRs are very close. The coupling between two elements is much enhanced for axial configuration, the interaction of the SRRs with second nearest neighbors becomes important, but if they are sufficiently far from each other, then only interaction between nearest neighbors needs to be taken into account. Here we assume there is only nearest-neighbor interaction. The mutual inductance M can be positive or negative. For planar configurations because the magnetic field originating in a SRR changes its direction when crossing its neighbors, M is negative, but for axial configurations M is positive. We assume electromagnetic wave propagates in such SRRs array with magnetic component perpendicular to the SRRs plane and that the electric component is transverse to the slit. Normalizing the charge Q_n stored in the nth SRR, $Q_n=(C_l d_g E_c)q_n$, and the

*yyzhu@nju.edu.cn

current I_n circulating in the nth SRR $I_n=(C_l d_g E_c \omega_l) i_n$, and the time to $(LC_l)^{1/2}t$, where C_l is the linear capacitance, d_g is the size of the slit, and $\omega_l=(LC_l)^{-1/2}$, q_n and i_n are found to obey the evolution equations as following [18]:

$$\frac{d^2}{dt^2}(\lambda q_{n-1} - q_n + \lambda q_{n+1}) - q_n + \frac{\alpha}{3\epsilon_l} q_n^3 + \mathcal{E}(t) = \gamma \frac{dq_n}{dt}, \quad (1)$$

$$i_n = \frac{dq_n}{dt}, \quad (2)$$

where $\lambda=M/L$ denotes the intersite coupling constant, $\gamma=RC_l\omega_l$ is the loss coefficient, and $\mathcal{E}$ is the electromotive force induced in each SRR due to the applied field. In the following we neglect losses by setting $\gamma=0$. By substituting a plane wave with the form $\sim\exp i(knd_0-\omega t)$ into Eqs. (1) and (2), we get the linear dispersion relation of magnetoinductive waves in such a system:

$$\omega = (1 - 2\lambda \cos kd_0)^{-1/2}. \quad (3)$$

Equation (3) shows there are lower cutoff frequency $\omega_{min}=\omega(k=\pi/d_0)=(1+2|\lambda|)^{-1/2}$ and higher cutoff frequency $\omega_{max}=\omega(k=0)=(1-2|\lambda|)^{-1/2}$, which are decided by the parameter λ describing the properties of the system. The physically meaningful range for λ is $\lambda \leq 1/2$. MI waves are forward in the axial configuration ($\lambda>0$) with codirectional phase and group velocities and backward in the planar configuration ($\lambda<0$), with phase and group velocities in the opposite directions [12]. The most interesting point of the spectrum is $k=\pi/(2d_0)$, which corresponds to a pair of equivalent oscillate eigenmodes: at $k=\pi/(2d_0)$, there are no current in the even SRRs and the current in the odd ones circulate with the opposite phases at the frequency $\omega=1$, or vice versa, there are no current in the odd SRRs but the current in the even ones circulate with the opposite phases at the same frequency. Because of the nonlinearity of Eq. (1), a symmetry breaking occurs between these two equivalent linear eigenmodes and a frequency gap will open at $k=\pi/(2d_0)$. Let us introduce two functions for the odd and even charge stored in the SRRs, i.e., $q_{2j}=v_n$, for $n=2j$ (even sites) and $q_{2j+1}=w_n$ (odd sites), where n is the index of the nth cell. Then Eq. (1) can be written to two coupling nonlinear equations:

$$\frac{d^2}{dt^2}(\lambda w_{n-1} - v_n + \lambda w_n) - v_n + \frac{\alpha}{3\epsilon_l} v_n^3 + \mathcal{E} = 0, \quad (4)$$

$$\frac{d^2}{dt^2}(\lambda v_{n-1} - w_n + \lambda v_n) - w_n + \frac{\alpha}{3\epsilon_l} w_n^3 + \mathcal{E} = 0. \quad (5)$$

By letting $(v_n,w_n)=(v_0,w_0)\exp[i(knd-\omega t)]+\text{c.c.}$, where $d=2d_0$ is the spacing of unite cell and v_0 and w_0 are real constants, using a rotating wave approximation, i.e., retaining only first-order harmonics, we can find the continuum wave spectrum of the nonlinear system as

$$(\omega^2 - 1 + \alpha v_0^2/\epsilon_l)(\omega^2 - 1 + \alpha w_0^2/\epsilon_l) = 4\lambda^2\omega^4 \cos^2 d_0 k. \quad (6)$$

The above nonlinear continuous wave spectrum incorporates the amplitude dependence of the wave frequency. At $k=\pi/(2d_0)$, this dispersion relation exhibits a nonlinear-induced gap

$$\Delta\omega^2 = |\omega_1^2 - \omega_2^2| = \left| \frac{\alpha}{\varepsilon_l}(v_0^2 - w_0^2) \right|. \quad (7)$$

The gap frequencies, $\omega_1^2=1-\alpha v_0^2/\epsilon_l$ and $\omega_2^2=1-\alpha w_0^2/\epsilon_l$, correspond to two modes, $v_n=(-1)^n v_0 \exp(-i\omega_0 t)$ and $w_n=0$, and $w_n=(-1)^n w_0 \exp(-i\omega_0 t)$ and $v_n=0$, which are different provided $v_0^2 \neq w_0^2$. The frequency gap in the continuum spectrum, resulting from the symmetry breaking between two equivalent linear eigenmodes at $k=\pi/(2d_0)$, may result in the wave localization with the frequency lying within the gap.

III. GAP SOLITONS IN ONE-DIMENSIONAL SRRS ARRAYS

We first consider the case with applied field $\mathcal{E}=0$. In the vicinity of the point $k=\pi/(2d_0)$, using quasidiscreteness approximation we make the antsatz

$$v_n = (-1)^n[V(\xi_n,\tau)\exp(i\omega_0 t) + V^*(\xi_n,\tau)\exp(-i\omega_0 t)], \quad (8)$$

$$w_n = (-1)^n[W(\xi_n,\tau)\exp(i\omega_0 t) + W^*(\xi_n,\tau)\exp(-i\omega_0 t)], \quad (9)$$

where $\xi_n=\varepsilon^2 nd$, $\tau=\varepsilon^2 t$ are slow variables, and ε is a small parameter. Substituting Eqs. (8) and (9) into Eqs. (4) and (5), retaining to order $O(\varepsilon^3)$ and making rotating-wave approximation, one can obtain

$$i\omega_0 \frac{\partial V}{\partial t} - \lambda d_0 \omega_0^2 \frac{\partial W}{\partial x} - \frac{\alpha}{2\epsilon_l}|V|^2 V = 0, \quad (10)$$

$$i\omega_0 \frac{\partial W}{\partial t} + \lambda d_0 \omega_0^2 \frac{\partial V}{\partial x} - \frac{\alpha}{2\epsilon_l}|W|^2 W = 0, \quad (11)$$

with $x=nd$, when returning to the original variables. Equations (10) and (11) are two coupled nonlinear differential equations. Stationary solutions of Eqs. (10) and (11) can be obtained in the form $(V,W)=[f_1(x),f_2(x)]e^{-i\Omega t}$, where Ω is an arbitrary real parameter and f_1 and f_2 is real [7]. Equations (10) and (11) then transform into

$$\frac{df_1}{dz} = -\omega_0 \Omega f_2 + \nu f_2^3, \quad (12)$$

$$\frac{df_2}{dz} = \omega_0 \Omega f_1 - \nu f_1^3, \quad (13)$$

with $z=x/\lambda d_0 \omega_0^2$ and $\nu=\alpha/(2\epsilon_l)$. It is not difficult to get a conservative quantity of Eqs. (12) and (13):

$$E = -\frac{1}{2}\omega_0 \Omega (f_1^2 + f_2^2) + \frac{1}{4}\nu(f_1^4 + f_2^4). \quad (14)$$

Thus Eqs. (12) and (13) describe the dynamics of a Hamiltonian system with one degree of freedom. The exact solution can be obtained by introducing an auxiliary function $g=f_1/f_2$ which satisfies

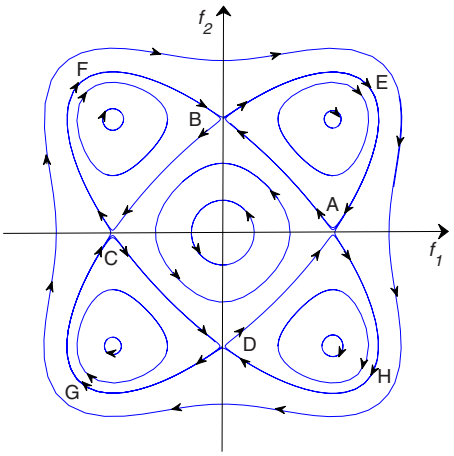

FIG. 1. (Color online) The phase portrait for the case $\Omega<0$, $\nu<0$ (self-defocusing media).

$$\left(\frac{dg}{dz}\right)^2 = \omega_0^2\Omega^2(1+g^2)^2 + 4\nu E(1+g^4), \tag{15}$$

and f_1 and f_2 may be found by the relation

$$f_2^2 = \frac{1}{\nu(1+g^4)}\{\omega_0\Omega(1+g^2) \pm [\omega_0^2\Omega^2(1+g^2)^2 + 4E\nu(1+g^4)]^{1/2}\}, \tag{16}$$

with $f_1=gf_2$. It is helpful to use the method of qualitative analysis of dynamical systems and consider possible solutions of Eqs. (12) and (13) in the phase plane (f_1,f_2). Attention should be paid to separatrixes, which correspond to different kinds of soliton solutions. As a dynamical system, Eqs. (12) and (13) have five center points (0, 0), $(\pm f_0, \pm f_0)$ on the phase plane with $f_0=(\omega_0\Omega/\nu)^{1/2}$. If the embedded media is self-focusing, $\nu>0$, the solution f_0 exists when the arbitrary parameter $\Omega>0$. For self-defocusing media, $\nu<0$, Ω is needed to be negative. The phase portraits of the system have been exhibited in Fig. 1(a). It can be seen in the figure that $A(f_0,0)$, $B(0,f_0)$, $C(-f_0,0)$, and $D(0,-f_0)$ are saddle points. All the separatrix curves connecting a pair of the neighboring saddle points are heteroclinic orbits. On these separatrix curves $E=-\omega_0^2\Omega^2/4\nu$. The solutions corresponding to this orbits can be obtained by integrating Eq. (15). We have

$$g = \delta_0 \exp(\delta_1\sqrt{2}\omega_0\Omega z), \tag{17}$$

$$f_2 = \delta_3\left(\frac{\Omega\omega_0}{\nu}\right)^{1/2}\exp(-\delta_1\omega_0\Omega z/2) \times\left[\frac{2\cosh(\sqrt{2}\omega_0\Omega z)+\sqrt{2}\delta_0\delta_2}{2\nu\cosh(2\sqrt{2}\omega_0\Omega z)}\right]^{1/2}, \tag{18}$$

$$f_1 = gf_2, \tag{19}$$

where $\delta_j(j=0,1,2,3)=\pm 1$. By choosing the values of $\delta_j(j=0,1,2,3)$, we can obtain different possible kinds of noncutoff kink solutions. The solutions correspond to different separatrix curves shown in Fig. 1. For example, the orbit AB corresponds to $\delta_0=\delta_3=1$ and $\delta_1=\delta_2=-1$, and for the orbit BEA, $\delta_0=1,\delta_1=\delta_2=\delta_3=1$. The distributions for the orbits AB and BEA have been shown in Figs. 2(a) and 2(b). The other solutions correspond to the separatrixies BC, CFB, CD, DGC, and AHD can be obtained by symmetry.

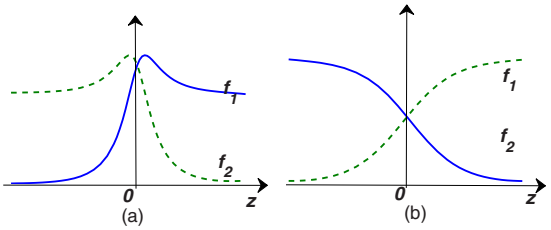

FIG. 2. (Color online) The even and odd components for soliton solutions corresponding to the cases (a) separatrix curve BEA in Fig. 1(b) separatrix curve AB in Fig. 1.

Next, we consider self-induced gap solitons for SRR arrays which are subjected to the external driving $\mathcal{E}$ due to the applied field. In order to generate gap solitons in this case we start by solving Eqs. (4) and (5). Further we assume that the applied field $\mathcal{E}=\mathcal{E}_1\cos(\omega_e\tau)$, $\mathcal{E}_1=\varepsilon^3\mathcal{E}_0$, and $\omega_0-\omega_e=\epsilon^2\Delta\Omega$, which means the applied field is weak and the frequency of the applied field ω_e approaches ω_0. Substituting Eqs. (8) and (9) into Eqs. (4) and (5), we obtain

$$i\omega_0\frac{\partial V}{\partial\tau} - \lambda d_0\omega_0^2\frac{\partial W}{\partial\xi_n} - \frac{\alpha}{2\epsilon_l}|V|^2V + \frac{\mathcal{E}}{4}(-1)^n e^{-i\Delta\Omega\tau} = 0, \tag{20}$$

$$i\omega_0\frac{\partial W}{\partial\tau} + \lambda d_0\omega_0^2\frac{\partial V}{\partial\xi_n} - \frac{\alpha}{2\epsilon_l}|W|^2W + \frac{\mathcal{E}}{4}(-1)^n e^{-i\Delta\Omega\tau} = 0. \tag{21}$$

Then making transformation

$$[V(\xi_n,\tau),W(\xi_n,\tau)] = [f_1(\xi_n,\tau),f_2(\xi_n,\tau)]\exp(-i\Delta\Omega t)(-1)^n, \tag{22}$$

Equations (20) and (21) are changed to

$$i\omega_0\frac{\partial f_1}{\partial t} - \lambda d_0\omega_0^2\frac{\partial f_2}{\partial x} + \omega_0\Delta\Omega f_1 - \frac{\alpha}{2\epsilon_l}|f_1|^2f_1 + \frac{\mathcal{E}_0}{4} = 0, \tag{23}$$

$$i\omega_0\frac{\partial f_2}{\partial t} + \lambda d_0\omega_0^2\frac{\partial f_1}{\partial x} + \omega_0\Delta\Omega f_2 - \frac{\alpha}{2\epsilon_l}|f_2|^2f_2 + \frac{\mathcal{E}_0}{4} = 0. \tag{24}$$

Here we use the original variables. For nonpropagating solutions we can postulate that $\partial f_1/\partial t=\partial f_2/\partial t=0$, Eqs. (23) and (24) transform into

$$\frac{df_1}{dz} = -\omega_0\Delta\Omega f_2 + \nu f_2^3 - \frac{\mathcal{E}_0}{4}, \tag{25}$$

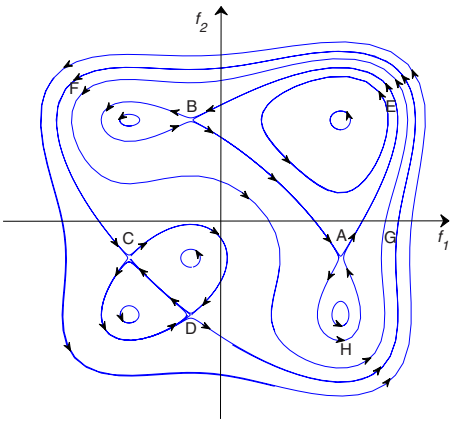

FIG. 3. (Color online) The phase portrait for the case $\Delta\Omega>0$, $\nu>0$ with applied field $\mathcal{E}$.

$$\frac{df_2}{dz} = \omega_0 \Delta\Omega f_1 - \nu f_1^3 + \frac{\mathcal{E}_0}{4}. \tag{26}$$

A conserved quantity from Eqs. (25) and (26) can be obtained

$$E = -\frac{1}{2}\omega_0\Omega(f_1^2+f_2^2) + \frac{1}{4}\nu(f_1^4+f_2^4) - \frac{\mathcal{E}_0}{4}(f_1+f_2). \tag{27}$$

Since it is difficult to obtain analytical solutions of Eqs. (25) and (26), we use the method of qualitative analysis and numerical simulation. In the simulation, ω_e, the external drive frequency, is an adjustable parameter so $\Delta\Omega>0$ and $\Delta\Omega<0$ are both possible. An analysis shows if $\Delta\Omega$ and ν have different sign, i.e., $\mathrm{sgn}(\alpha)\mathrm{sgn}(\Delta\Omega)<0$, the system has unique center point, no localized structure can be found. But for $\mathrm{sgn}(\alpha)\mathrm{sgn}(\Delta\Omega)>0$, localized structure such as gap solitons is possible. One case is the embedded material is self-focusing ($\alpha=1$) and the external drive frequency $\omega_e<\omega_0$, and another case is the embedded material is self-defocusing ($\alpha=-1$) and $\omega_e>\omega_0$. As a dynamical system, Eqs. (25) and (26) have five centers at $(\tilde{f}_0,\tilde{f}_0)$, $(-\tilde{f}_0/2-\rho/2,-\tilde{f}_0/2-\rho/2)$, $(-\tilde{f}_0/2+\rho/2,-\tilde{f}_0/2-\rho/2)$, $(-\tilde{f}_0/2-\rho/2,-\tilde{f}_0/2+\rho/2)$, $(-\tilde{f}_0/2+\rho/2,-\tilde{f}_0/2+\rho/2)$, and four saddle points at $A(-\tilde{f}_0/2+\rho/2,\tilde{f}_0)$, $B(\tilde{f}_0,-\tilde{f}_0/2+\rho/2)$, $C(-\tilde{f}_0/2-\rho/2,\tilde{f}_0)$, $D(\tilde{f}_0,-\tilde{f}_0/2-\rho/2)$ with $\tilde{f}_0=(-\alpha+\beta)^{1/3}-(\alpha+\beta)^{1/3}$, $\rho=(-3\tilde{f}_0^2+4\omega_0\Delta\Omega/\nu)^{1/2}$, $\alpha=\mathcal{E}_0/(2\nu)$, and $\beta=[\mathcal{E}_0^2/(16\nu^2)+4\omega_0^3\Delta\Omega^3/27]^{1/2}/2$. The phase portrait for $\alpha=1$, $\Delta\Omega>0$ has been sketched in Fig. 3. To find the gap solitons with applied field, we pay much attention to the separatrix curves on the phase plane. There are two different types of separatrix curves unlike the case without applied field. One is a heteroclinic orbit, i.e., *AEB*, *BA*, *DGFC*, and the other one is a homoclinic orbit, i.e., *AHA*. The numerical simulation corresponding to separatrixes *AHA* and *DGFC* have been depicted in Figs. 4(a) and 4(b). By using Eqs. (8), (9), and (22), the charge stored in SRR varies

$$v_n = f_1 \exp(i\omega_e t) + f_1^* \exp(-i\omega_e t), \tag{28}$$

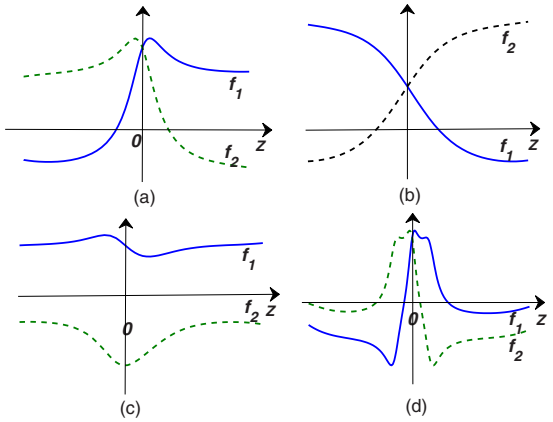

FIG. 4. (Color online) The even and odd components for soliton solutions corresponding to the cases (a) heteroclinic orbit *AEB*, (b) heteroclinic orbit *BA*, (c) homoclinic orbit *AHA*, and (d) heteroclinic orbit *DGFC* in Fig. 3.

$$w_n = f_2 \exp(i\omega_e t) + f_2^* \exp(-i\omega_e t). \tag{29}$$

From Eqs. (28) and (29) we can see due to the external field the variation frequency of current in SRRs is the same with external field frequency, and the even (or odd) SRRs now have the same phase differently from the case without external field. We perform numerical simulations using Eq. (1) with the initial conditions (17)–(19), (28), and (29). A lattice of $N=100$ SRRs with period boundary conditions is investigated. Typical localized structures are shown in Figs. 5(a) and 5(b). Figure 5(a) depicts noncutoff kinks without applied field. The parameters are chosen as $\lambda=0.15$, $\epsilon_l=2$, $\alpha=1$, and $\Omega=0.1$. We find that the kinks evolute for long time intervals (over 10^4 oscillation period) without observing any significant change in the shape. Moreover, we checked the case which the SRR arrays are subjected to the weak external driving force shown in Fig. 5(b), i.e., $\mathcal{E}_0=0.0024$, $\omega_e=0.98\omega_0$, and the localized structure also seems stable. Without external field, the nearest-neighbor even (or odd) SRRs

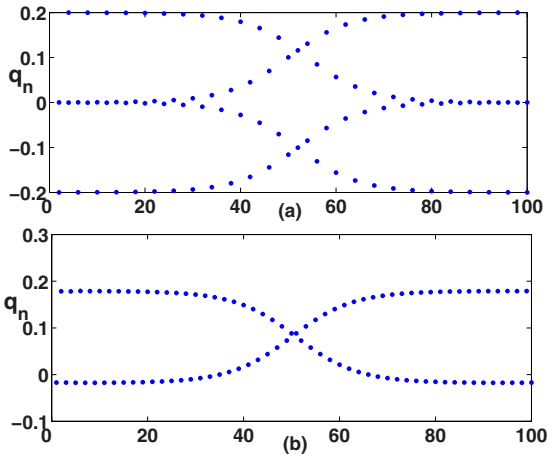

FIG. 5. (Color online) The charge distribution for $\lambda=0.15$, $\epsilon_l=2$, $\alpha=1$, and $\Omega=0.1$ corresponding to (a) the separatrix curve *AB* in Fig. 2(b) without external field and (b) the separatrix curve *AEB* in Fig. 4(c) with external field, $\mathcal{E}_0=0.0024$ and $\omega_e=0.98\omega_0$.

oscillate with opposite phase, but when the external field is considered, the ones oscillate with the same phase and the amplitude are also changed. The simulations based on the discrete model show fairly good agreement with the analytical expressions derived from the quasidiscreteness approximation of that model. The nonlinear excitations such as kinks and localized structures in 1D discrete arrays original from the balance between the effect of dispersion (due to the periodic location of SRRs) and nonlinearity (due to the permittivity dependence of the electric field). For our nonpropagating localized modes, the localized nonlinear magnetoinductive waves have a spatial extension, the current in each SRRs oscillates with their own amplitude and the profile of localized modes cannot propagate.

Noticing that in the experimental 1D SRRs array system, the self-inductance of a circular SRR is determined by the $L=\mu_0 a[\ln(16a/h)-1.75]$ which the parameter a is radius and h is circular cross section of diameter. The expression for the mutual inductance between two SRRs can be calculated by means of a simple approximation as $M \simeq \mu_0 \pi a^4/4d_0^3$ for planar geometry. For axial geometry the mutual inductance is $M \simeq (\pi/2)\mu_0 a(a/d_0)^3$. The coupling parameter $\lambda = M/L$ calculated in the axial geometry is twice as strong as planar geometry with the same separation distance d_0 approximately. Choosing $a=2.4$ μm, $h=1.1$ μm, and $d_0=4.3$ μm the resonance frequency for a single SRR is about 6.2 THz and the coupling parameter $\lambda \simeq 0.15$ for axial geometry [18,19]. The linear permittivity can be taken as $\epsilon_l=2$. These requirements can be easily realized in experiment. Although considerable theoretical study has been made for the gap solitons in discrete systems, there are only a few systems where gap solitons are easily and directly observed in controlled laboratory experiments [1]. Self-induced gap solitons as one of interesting localized structures first introduced by Kivshar in 1993 [7], only have been realized experimentally in pendulum lattice to our knowledge [22]. We wish the discrete array of nonlinear SRRs can be taken as a good system to realize self-induced gap solitons. Considering the size of each element and the distance between them can be easily controlled, the great flexibility of metamaterial engineering maybe provide such an opportunity. Moreover, with applied field more rich self-localized structures can be observed.

IV. CONCLUSIONS

In conclusion, we have analytically and numerically investigated the nonlinear localized structures in a one-dimensional SRRs arrays. The results show that the intrinsic interaction between SRRs can support self-induced gap solitons. One pattern is noncutoff kink. These localized structures appear due to the symmetry breaking between two equivalent linear eigenmodes at $q=\pi/(2d_0)$, i.e., due to a nonlinearity-induced frequency gap in continuum wave spectrum. The evolution of these localized structures is studied in the phase plane and their analytical and numerical results are proposed. Applications of MI waves have been reported for delay lines [23], phase shifters [24], and microwave lenses [25], then we expect our studies will further inspire the MMs application in nonlinear regime.

ACKNOWLEDGMENTS

The work was supported by the State Key Program for Basic Research of China (Grant No. 2004CB619003) and the National Science Foundation of China (Grants No. 10523001 and No. 10874079).

[1] F. Lederer, G. I. Stegemanb, D. N. Christodoulides, G. Assanto, M. Segev, and Y. Silberberg, Phys. Rep. **463**, 1 (2008).
[2] A. J. Sievers and S. Takeno, Phys. Rev. Lett. **61**, 970 (1988).
[3] A. J. Heeger, S. Kivelson, J. R. Schrieffer, and W. P. Su, Rev. Mod. Phys. **60**, 781 (1988).
[4] G. Huang and Z. Jia, Phys. Rev. B **51**, 613 (1995).
[5] E. Trias, J. J. Mazo, and T. P. Orlando, Phys. Rev. Lett. **84**, 741 (2000).
[6] W. Chen and D. L. Mills, Phys. Rev. Lett. **58**, 160 (1987).
[7] Yu. S. Kivshar, Phys. Rev. Lett. **70**, 3055 (1993).
[8] J. B. Pendry, A. J. Holden, D. J. Robbins, and W. J. Stewart, IEEE Trans. Microwave Theory Tech. **47**, 2075 (1999).
[9] D. R. Smith, W. J. Padilla, D. C. Vier, S. C. Nemat-Nasser, and S. Schultz, Phys. Rev. Lett. **84**, 4184 (2000).
[10] J. B. Pendry and D. R. Smith, Phys. Today **57** (6), 37 (2004).
[11] E. Shamonina, V. A. Kalinin, K. H. Ringhofer, and L. Solymar, Electron. Lett. **38**, 371 (2002).
[12] E. Shamonina, V. A. Kalinin, K. H. Ringhofer, and L. Solymar, J. Appl. Phys. **92**, 6252 (2002).
[13] A. A. Zharov, I. V. Shadrivov, and Y. S. Kivshar, Phys. Rev. Lett. **91**, 037401 (2003).
[14] S. O'Brien, D. McPeake, S. A. Ramakrishna, and J. B. Pendry, Phys. Rev. B **69**, 241101(R) (2004).
[15] M. Lapine, M. Gorkunov, and K. H. Ringhofer, Phys. Rev. E **67**, 065601(R) (2003).
[16] I. V. Shadrivov, S. K. Morrison, and Y. S. Kivshar, Opt. Express **14**, 9344 (2006).
[17] I. V. Shadrivov, A. N. Reznik, and Y. S. Kivshar, Physica B **394**, 180 (2007).
[18] N. Lazarides, M. Eleftheriou, and G. P. Tsironis, Phys. Rev. Lett. **97**, 157406 (2006).
[19] M. Eleftheriou, N. Lazarides, and G. P. Tsironis, Phys. Rev. E **77**, 036608 (2008).
[20] I. V. Shadrivov, A. A. Zharov, N. A. Zharova, and Y. S. Kivshar, Photonics Nanostruct. Fundam. Appl. **4**, 69 (2006).
[21] I. Kourakis, N. Lazarides, and G. P. Tsironis, Phys. Rev. E **75**, 067601 (2007).
[22] B. Denardo, B. Galvin, A. Greenfield, A. Larraza, S. Putterman, and W. Wright, Phys. Rev. Lett. **68**, 1730 (1992).
[23] M. J. Freire, R. Marques, F. Medina, M. A. G. Laso, and F. Martin, Appl. Phys. Lett. **85**, 4439 (2004).
[24] I. S. Nefedov and S. A. Tretyakov, Microwave Opt. Technol. Lett. **45**, 98 (2005).
[25] M. J. Freire and R. Marques, Appl. Phys. Lett. **86**, 182505 (2005).